Surface modification of gold electrode with gold nanoparticles and mixed self-assembled monolayers for enzyme biosensors

Byung-Wook Park*, Dong-Shik Kim*, and Do-Young Yoon**,†

*Department of Chemical & Environmental Engineering, University of Toledo, Toledo, OH 43606, U.S.A.
**Department of Chemical Engineering, Kwangwoon University, Seoul 139-701, Korea

Abstract−This paper describes the development and evaluation of a generic method for the immobilization of enzymes onto a gold electrode and its application to amperometric biosensors. The surface of the gold electrode was modified with gold nano-particles (AuNP) and mixed self-assembled monolayers (SAMs) to form an enzyme biosensor matrix. Horseradish peroxidase (HRP) was immobilized on the modified surface to form a biosensor matrix on a gold electrode. After the deposition of gold nano-particles on a bare gold surface, the AuNP-deposited gold electrode and a bare electrode were compared for the surface area and electric current using AFM and cyclic voltammetry (CV). The AuNP strongly adhered to the surface of the gold electrode, had uniform distribution and was very stable. A mixed SAM, composed of two different monolayer molecules, dithiobis-N-succinimidyl propionate (DTSP) and inert tetradecane-1-thiol (TDT), was formed using reductive desorption technique and cyclic voltammetry was used to verify the formation of mixed deposition. First, 3-mercaptopropionic acid (MPA) and TDT were deposited with a specified deposition ratio between the two components. Then, MPA was desorbed by applying electric potential to the surface. Finally, DTSP was deposited where MPA was. The ratios of 20 : 80 and 50 : 50 between MPA and TDT were examined, and differences in the CV responses were discussed. HRP was immobilized on the mixed SAM surface. The investigated method is regarded as an effective way for stable enzyme attachment, while the presence of gold nanoparticles provides enhanced electrochemical activity; it needs very small amounts of samples and enzymes and the SAM matrix helps avoid enzyme leaking. It is interesting that the mixed SAM shows unique CV characteristics compared to the uni-molecular SAMs. The reaction kinetics of the SAM-immobilized enzyme is discussed with the CV results and is observed to obey the Michaelis-Menten equation.

Key words: Gold Nano-particles, Mixed Self-assembled Monolayer, Reductive Desorption, Amperometric Sensor, Horseradish Peroxidase, Enzyme Sensor

INTRODUCTION

An enzyme biosensor uses the reaction between enzymes and target analytes that produces a signal proportional to the target analyte concentration. The signal is a result of a change in proton concentration, light emission, absorption or reflectance, heat emission, etc. A transducer converts this signal into a measurable response, such as current, potential, temperature change, or absorption of light through electrochemical, thermal, or optical means. This signal can be further amplified, processed, or stored for later analyses.

Because of their specificity and catalytic advantages, enzymes have found widespread use as sensing elements in biosensors. Amperometric biosensors are based on the redox reaction of enzymes that can react with fatty acids, sugars, amino acids, aldehydes, and phenols [1]. Due to the advantages of high redox potential, low interferences, and good regenerability, peroxidase enzymes such as horseradish peroxidase (HRP) and soybean peroxidase (SBP) are becoming more popular for directly measuring hydrogen peroxide or organic chemicals [2]. Peroxidases are sometimes used with antibody, DNA, or aptamer to measure food toxins [3], toxic chemicals [4,5], environmental hormones [6], and pathogens [7].

In the matrix layer for the biosensor, HRP is either directly immobilized on the electrode surface as illustrated in Fig. 1(a), or attached to the self-assembled monolayers (SAMs) bound to the electrode's surface (Fig. 1(b)). Enzymes are sometimes encapsulated or entrapped in polymer gels as shown in Fig. 1(c). When enzymes are covalently immobilized onto the surface of an electrode, enzymes may lose their activity due to the deformation and/or restrictions on orientation of active sites. Entrapment of enzymes may suffer from reduced mass and signal transfer rates. On the other hand, immobi-
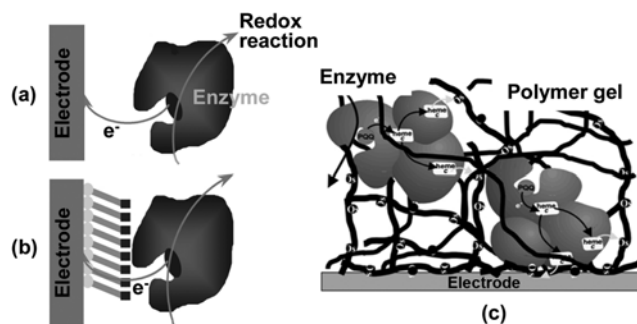
Fig. 1. Enzyme immobilization methods: (a) on the self-assembled monolayer, (b) direct adsorption, and (c) entrapment in polymer gel.

†To whom correspondence should be addressed.
E-mail: yoondy@kw.ac.kr

lization of enzymes on SAMs offers the possibility of controlling the orientation, distribution, and spacing of the enzymes while reducing the possibility of deformation of enzymes and of reduction of mass and electron transfer rates. SAM surfaces are quasi-crystalline, stable, and reproducible. SAMs are becoming important in sensor research due to the thermodynamic stability and easy control of chemical properties by varying the functional groups. Primarily, they provide specific binding sites for immobilizing various sensing elements.

Most SAMs are chemically inactive, but they act as electron tunneling wires, which may affect electron transfer rate between the enzyme and electrode. Packing density of SAM is one of the important design factors for optimizing the sensitivity and rate of a sensor. If they are too densely packed, there will be more bonding sites for the sensing elements to bind with, and more enzymes will be possibly immobilized, which may increase the signal generation. However, the dense packing of the linking agents will decrease the electron transfer rate, which will delay and attenuate the sensing process. If the packing is insufficient, however, the SAM is not stable, and not enough enzymes can be immobilized. Likewise, the SAM chain length also affects the surface coverage and electron transfer rate. Mixed SAMs of long and short chains are reported to show better electron transfer rates than unicomponent SAMs due to the flexibility of redox species distribution at the SAM interface [8]. When part of a COOH-thiol SAM was substituted with OH-thiols to form a mixed layer of COOH- and OH-functionalized SAMs, more than 1,000 times higher electron transfer rates were observed [9].

Another advantage of the binary SAMs is the possibility of better control of non-specific adsorption. Not only for enzymatic amperometric biosensors, but also for many other types of sensor matrices such as antibodies, DNAs, or aptamers, in electrochemical or photometric biosensors, binary SAMs can be useful for reducing non-specific adsorption. Non-specific adsorption of proteins from complex sample matrices, such as blood, environmental, or other clinical samples, is usually the major factor that limits the sensitivity. By employing two different self-assembled monolayers, a binary SAM can reduce non-specific adsorption of other molecules [10].

In this paper, first the gold surface of an electrode is modified with gold nano-particles (AuNP) to enhance the surface area. Then, for the SAM formation on the AuNP-modified surface, the SAM thickness and density are controlled using a mixture of two different SAMs. Atomic force microscopy (AFM), cyclic voltammetry (CV), electrochemical impedance spectroscopy (EIS), and scanning electron microscopy (SEM) are used to characterize the nanoparticle-modified gold surface and SAMs. Enzyme kinetics are analyzed using the CV data.

EXPERIMENTAL METHODS

1. Preparation of Gold Electrode

Gold electrodes were purchased from Gamry Instruments, USA. Before the surface modification, they were treated by piranha solution (a mixture with 3 : 1 of concentrated sulfuric acid and 30% hydrogen peroxide) for 10 minutes. Great caution was taken because piranha solution is extremely reactive with organic materials. Gold electrodes were mechanically polished with 1.0, 0.5, 0.3, and 0.05 mm sizes of alumina suspensions on a polishing microcloth (Bue-

hler, USA). The polished electrodes were sonicated in water and alcohol for 10 minutes. According to the manual provided by the manufacturer, the electrodes were electrochemically cleaned by potential scanning from −0.2 to 1.5 V in 0.05 M sulfuric acid at a scan rate of 50 mV/s until reproducible gold oxide stripping peaks were obtained.

2. Gold Electrode Surface Modification with Gold Nano-particles

The pretreated clean gold electrodes were immersed in 0.1 M KNO$_3$ containing 1 or 3 mM HAuCl$_4$ solution. Electrochemical deposition of gold nano-particles on a planar gold electrode was carried out at the working potential of −200 mV vs. Ag|AgCl in a saturated KCl solution for 22, 110, 330, and 550 seconds. The morphology of the samples was observed by using SEM, and electric current responses were measured with cyclic voltammetry.

3. SAM Immobilization and Reductive Desorption

Thiol self-assembled monolayer immobilization is a well established method. In this study, dithiobis-N-succinimidyl propionate (DTSP) was used in a dimethyl sulfoxide (DMSO) solution. DTSP is commonly used for SAMs for its distinctive surface properties, such as hydrophilicity, wettability, chemical reactivity, and an affinity towards positively charged proteins, e.g., cytochrome c [11]. Single component SAMs were prepared by immersing the gold substrate into a 1 mM DTSP in an ethanol solution for 24 h.

For the binary-SAM immobilization, first 3-mercaptopropionic acid (MPA) and tetradecane-1-thiol (TDT) were used according to Hobara et al. [12]. This combination was chosen because MPA has a lower redox potential than TDT, which means MPA can be easily eliminated by reductive desorption leaving TDT intact. DTSP replaced the positions where MPA was desorbed. DTSP forms a covalent bond with the amino groups (reactive lysine residues) of HRP while TDT does not, so that HRP may attach to DTSP only. Two-component thiol solutions were prepared by mixing 1 mM ethanol solutions of MPA and TDT at various ratios while keeping the total concentration of the binary SAMs at 1 mM. The binary SAMs of MPA and TDT, whose ratios were 50 : 50 and 80 : 20, were formed on the AuNP-modified electrodes by soaking the electrodes into the mixed thiol solution for 1 hr.

Binary SAM formation and reductive desorption procedures are as follows: First, the binary components of 3-mercaptopropionic acid (MPA) and TDT were adsorbed on the gold surface in an ethanol solution. The reductive desorption of MPA from the gold electrode
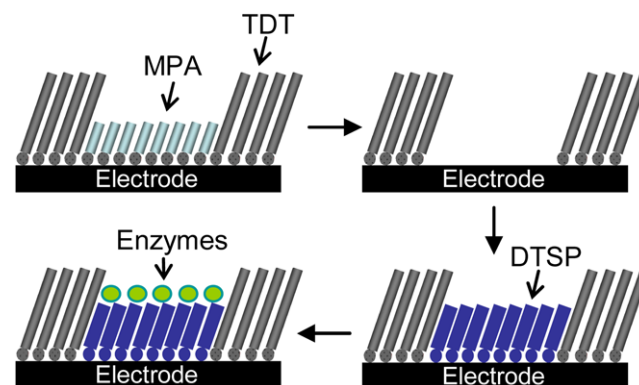

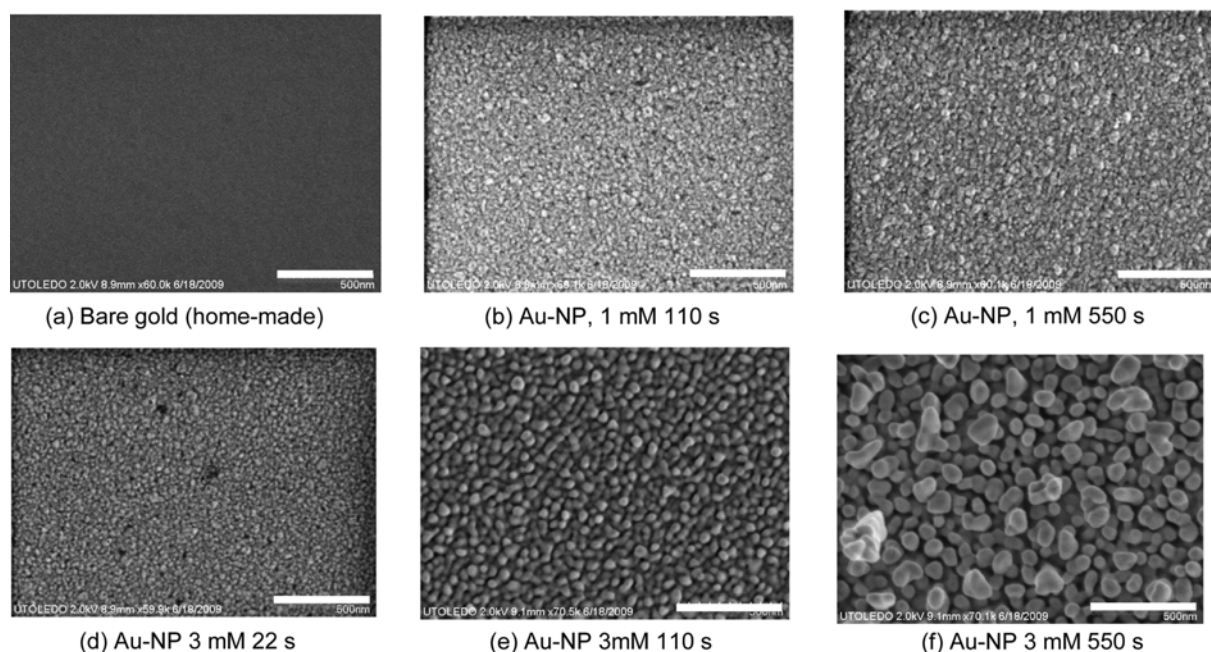Fig. 2. Schematic illustration of a binary mixed SAM formation.

Fig. 3. SEM images of (a) a home-made bare gold electrode, (b) AuNP modified electrodes at 1 mM for 110 s and (c) 550 s, (d) AuNP modified electrodes at 3 mM for 22 s and (e) 110 s and (f) 550 s respectively. Scale bar is 500 nm.

was performed in 0.5 M KOH solution. The adsorbed MPA in a phase-separated binary SAMs of MPA and TDT was selectively reduced by applying the potential of -1.2 V for 30 min. After reductive desorption of MPA, the sample with the TDT layer was immersed in the 1 mM DTSP solution to form DTSP layers on the MPA-desorbed sites. A schematic procedure of mixed SAM synthesis is illustrated in Fig. 2.

4. Enzyme Immobilization

Horseradish peroxidase was purchased from Sigma and stored as received at $-20\,^{\circ}$C. To immobilize the enzymes on top of SAMs, SAM-modified electrodes were immersed in 10 mM phosphate buffer (pH 7.0) solution containing HRP at a concentration of 1.0 mg/mL. The electrodes were kept in the enzyme solution for 24 hr at $4\,^{\circ}$C. The electrodes were stored in 10 mM PB solution at $4\,^{\circ}$C when not used, after subsequently rinsing the HRP/SAM-modified electrode with the PB solution.

5. Characterization

Cyclic voltammetry and electrochemical impedance spectroscopy (Reference 600 potentiostat, Gamry Instruments, USA) were used to analyze the electric responses of the SAMs-deposited gold electrodes. A cyclic voltammogram of the reductive desorption was recorded in 0.5 mol/dm^3 phosphate buffer solution using an Ag|AgCl electrode as the reference electrode and a platinum wire as the auxiliary electrode. Also, polycrystalline gold electrodes of 3 mm-diameter from Gamry Instruments, were employed as the working electrodes. CV curves of the SAM and HRP coated gold electrode (Au+SAM+HRP) and the reductively desorbed mixed SAMs and HRP on the gold electrode (Au+RD SAM+HRP) were compared. The CV curves were recorded at the scan rate of 100 mV/s for the reductive elimination. In each voltammogram, a downward peak of reductive desorption of SAM appeared around -50 mV. SEM (Hitachi S-4800, Japan) and AFM (Veeco Multimode Nanoscope IIIa, USA)

were used to characterize bare and modified gold surfaces.

RESULTS AND DISCUSSION

1. Surface Modification with Gold Nano-particles (AuNP)

Fig. 3(a) shows an SEM image of an untreated surface of the home-made electrode. Figs. 3(b) and (c) show the images of the gold nano-particle coating. The concentration of gold nano-particles was 1 mM, and the deposition process lasted for 110 and 550 seconds, respectively. The surface morphology became rough as the deposition lasted longer. Figs. 3(d), (e), and (f) show another set of experimental results for the deposition of gold nano-particles of 3 mM for different durations of deposition, 22, 110, and 550 seconds, respectively. The particle size grew larger as the duration increased. Higher concen-
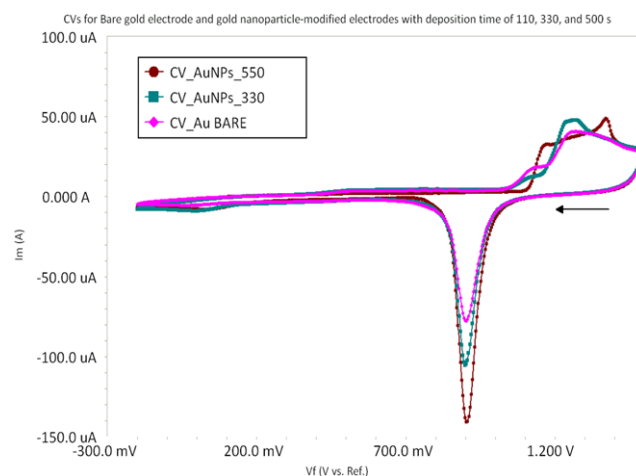

Fig. 4. CV responses for bare and nano-gold deposited electrodes.

trations of $HAuCl_4$ produced the coatings with larger size particles. The surface morphology difference made a significant impact on cyclic voltammetry of the gold electrode itself and moreover of the SAM-immobilized gold electrode also.

Fig. 4 shows the effect of surface morphology on cyclic voltammetric response. As the deposited gold particles grew larger, the current peaks negatively increased, which indicates less electron transfer resistance. The relative surface area could be evaluated from the coulombic integration of the cathodic peaks of gold oxide. Relative surface areas of the AuNP modified electrodes at various deposition times with the bare gold electrode were 1 (bare): 1.17 (330 s): 1.46 (550 s).

2. SAM and Enzyme Immobilization

AFM images of the immobilized SAM of DTSP and HRP enzymes on the plain gold surfaces are shown in Fig. 5. The surface became rougher as the enzymes were deposited. The thickness of the deposits also increased with the immobilization of the SAMs (Fig. 5(b)) and the enzymes (Fig. 5(c)). Moreover, observable increases of the surface roughness and thickness on top of the DTSP layer in Fig. 5(c) reflect the immobilization of HRP on the DTSP layer. Based on the AFM images, it has been shown that the surface roughness of a SAM-modified gold electrode is lessened than that of a bare gold electrode. Deposition of the enzymes seems obvious as the thickness and roughness increased as shown in Fig. 5(c).

Fig. 6 shows EIS results of these samples. Immobilization of substrates, e.g., enzymes, antigens/antibodies, DNA, or SAM on electrodes alters the interfacial capacitance and electron-transfer resistance of conductive electrodes. The impedance curve of the bare gold electrode shows a much smaller semicircular diameter, which indicates faster electron-transfer kinetics of a redox probe on the gold electrode. Also, it has been shown that the semicircular diameter enlarged with the immobilization of SAM and HRP, which implies a high electron-transfer resistance, possibly due to the increased thickness, compactness, and hydrophobic property of materials.

SAM deposition on the bare gold surface and the gold surface modified with gold nanoparticles (AuNP) shows different CV responses in Figs. 7(a) and (b). MPA has a short alkyl chain and a
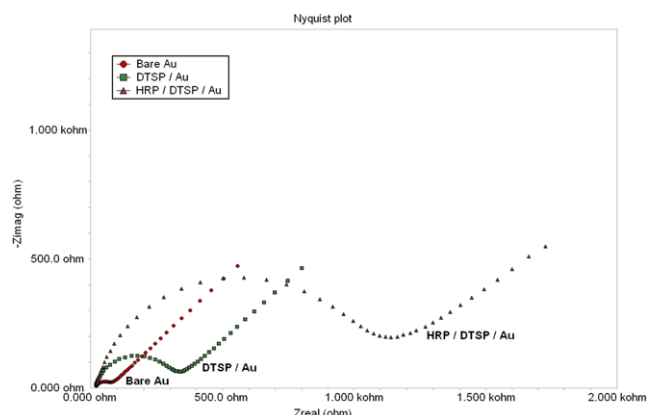

Fig. 6. Nyquist plots of EIS for the bare gold and the gold surfaces modified with the SAM and enzymes.

large functional group of COOH. On the bare gold electrode, the electron transfer of redox couples might largely decrease with binding of MPA SAM (Fig. 7(a)), but it decreased a little on the AuNP-modified electrode (Fig. 7(b)). It may possibly be explained that the dense MPA-absorbed layer on the bare gold electrode could facilitate the hydrogen bonding between MPA molecules after the layer formation, and as a result a large diffusion barrier was generated blocking the electron transfer. However, on the AuNP-modified electrode, the hydrogen bonding might be hard to occur, possibly due to the relatively less densely adsorbed SAM layer and more defects on the adsorbed SAM layer. Consequently, the diffusion of redox couples was comparably less blocked within the SAM bound to the gold nano-particle modified surface.

Fig. 8 shows the effect of mixed SAMs in cyclic voltammetry. These CV results clearly show that when the ratio of MPA and TDT was 50 : 50 (▲ and ▲ in Figs. 8(a) and (b), respectively) there were no oxidation and reduction peaks, suggesting the absence of major pinholes and vacancy spots in the monolayer. This means that the redox reaction could not readily take place in the electrode surface. As the TDT ratio decreased to 80 : 20 (▬ in Fig. 8(b)),
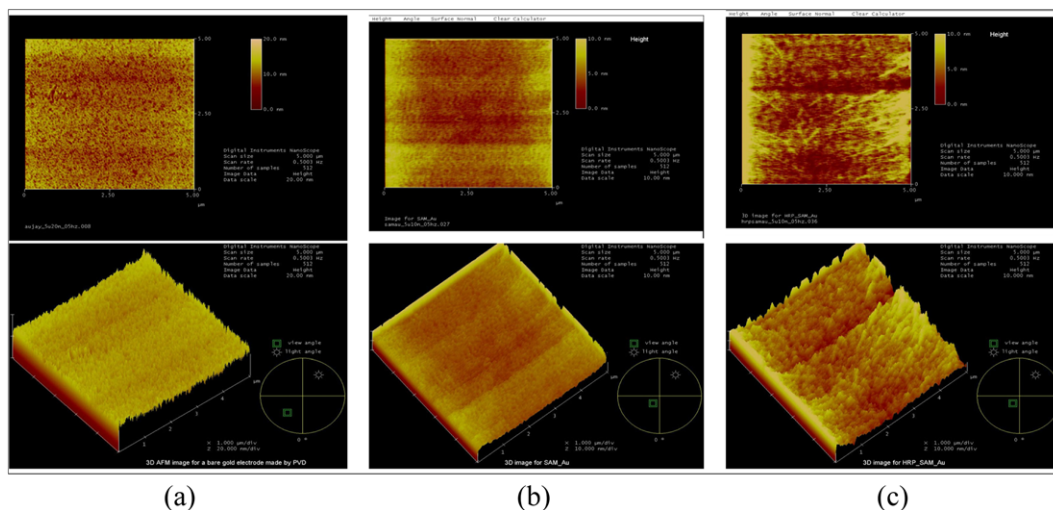

Fig. 5. AFM images of the surface topology of (a) gold electrode, (b) SAM immobilized on top of the gold coating, and (c) horse radish peroxidase attached to the SAM.
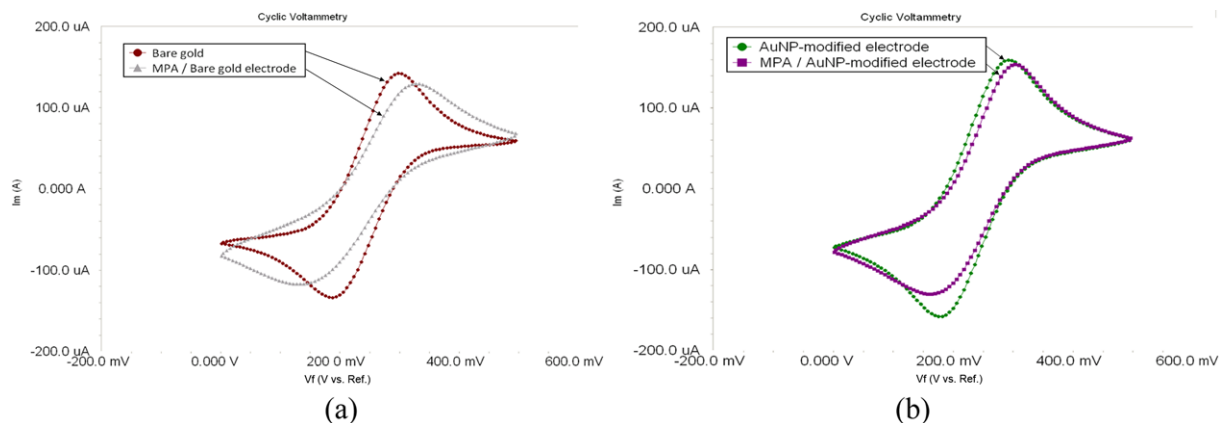
Fig. 7. (a) CVs for bare gold electrode and MPA-immobilized electrode. (b) CVs for gold nano-particle-modified (AuNP) electrode and MPA-immobilized onto an AuNP-modified electrode.
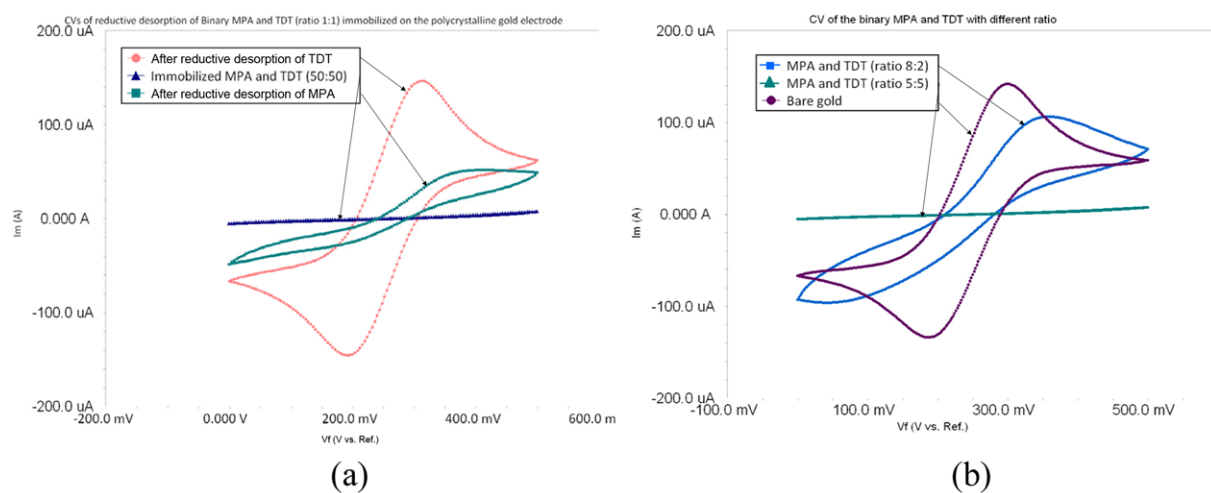

Fig. 8. (a) CV curves for MPA and TDT immobilized with a ratio of 50 : 50 on a gold electrode. (b) Comparison of CV's for different ratios of the binary system.
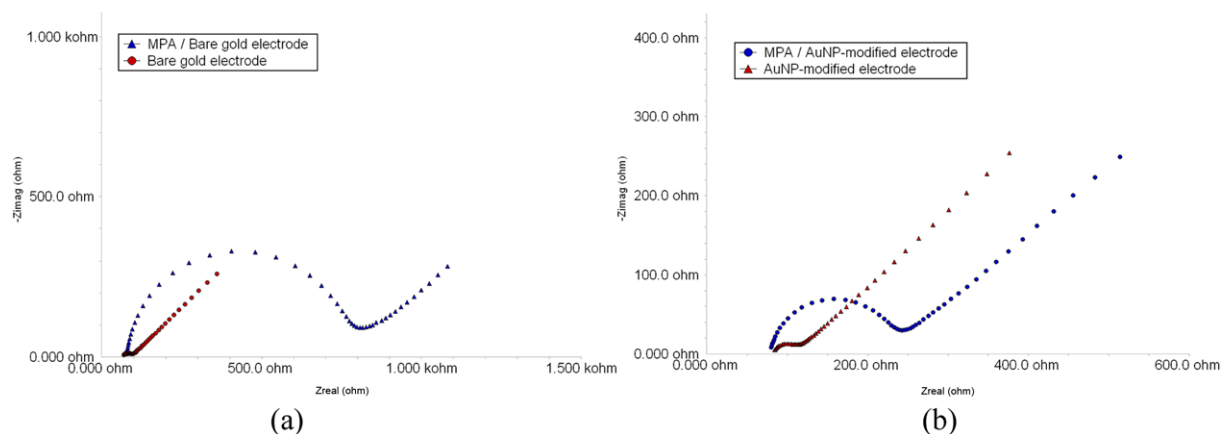

Fig. 9. Impedance measurement by EIS: (a) Bare gold electrode and MPA-immobilized on the bare gold electrode. (b) AuNP-modified electrode and MPA immobilized on it.

redox reversible peaks appeared, indicating that TDT had a higher chain-chain attractive interaction, and thereby they were densely immobilized on the gold surface. The same effect of TDT is shown

as the current response increased significantly when TDT was eliminated in Fig. 8(a) (—●—), which is comparable to the bare gold curve in Fig. 8(b) (—●—). After desorption of MPA, the CV exhibits the

character of a quasi-reversible system (━ in Fig. 8(a)). After desorption of TDT, it is clear that there are redox peaks, which means redox couples were reaching to the electrode surface.

The effect of the surface modification on the electron transfer is also clearly shown in the EIS results. Fig. 9 compares the two cases: (a) MPA immobilized on a bare electrode and (b) MPA immobilized on the surface modified electrode. The larger the circle, the greater the impedance is. Therefore, not only has the gold nanoparticle deposited electrode less resistance than a bare electrode, but also the SAM-immobilized one shows less resistance than the SAM-immobilized on a bare electrode.

3. Enzyme Reaction and Kinetics

The HRP enzymes immobilized on the DTSP SAM were tested with H_2O_2. CV results were obtained when H_2O_2 of 0.5mM was applied in a PB solution. As shown in Fig. 10(a), an enhancement in the reduction current was observed, demonstrating an electrocatalytic behavior of the HRP in response to the reduction of hydrogen peroxide.

The reaction rate, r_A, between the HRP and analyte was determined by using the reaction rate data obtained from cyclic voltammetry measurement. First, we measured amperometric responses of HRP with various concentrations of hydrogen peroxide, 0.05-0.9 mM, and 0.4-3.6 mM. Typical stepwise change of the current with respect to the H_2O_2 concentration was observed in Figs. 10(b) and (c), where the concentrations increased by 0.05 mM and 0.4 mM every minute up to 0.9 mM and 3.6 mM, respectively. The corresponding currents were measured and used for the calibration curves. These data of H_2O_2 concentrations versus currents were used to obtain

Fig. 10. (a) CV curves show the current change due to the redox reaction of HRP with H_2O_2, (b) Amperometric responses to H_2O_2 from 0.05 mM to 0.9 mM (18 increments), and (c) from 0.4 mM to 3.6 mM (10 increments).

basic reaction kinetics of HRP enzyme. A Michaelis-Menten type reaction rate equation [13] was derived as in Eq. (1):

$$I_{ss} = \frac{I_{max}[C]}{K_m + [C]} \tag{1}$$

where I_{max} and I_{ss} are the currents measured for enzymatic product detection under the conditions of substrate saturation and steady state, respectively, for a given substrate concentration, [C]. Kinetic parameters were estimated from the slope and intercept of the Lineweaver-Burke plot of the data [14] using Eq. (2):

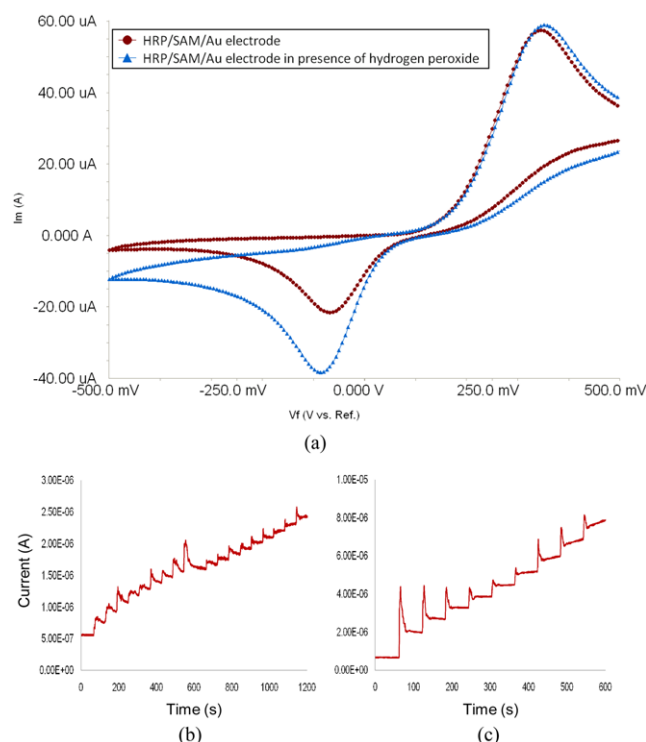$$\frac{1}{I_{ss}} = \left(\frac{K_m}{I_{max}}\right)\left(\frac{1}{C}\right) + \frac{1}{I_{max}} \tag{2}$$

K_m and I_{max} were determined from the slope and intercept by plotting 1/C versus $1/I_{ss}$; K_m=16.7 μM and I_{max}=833.33 nAmp. The higher low Mechaelis constant indicates that the low diffusion limitations inside the AuNP modified electrode play an important role. And the large I_{max} suggests that a large number of enzymes was immobilized on the SAMs. The presence of diffusion barriers is commonly encountered for enzymes entrapped within electrodeposited matrices; in this study, the measurement of the K_m and I_{max} values was reported apparently beneficial the enzyme biosensor.

CONCLUSIONS

The immobilization of enzymes on the surface of gold electrodes modified with gold nano-particles (AuNP) and mixed self-assembled monolayers (SAMs) to form an enzyme biosensor matrix has been investigated. From the foregoing results and discussion presented in the previous sections, the following conclusions can be drawn:

1. Deposition of gold nano-particles increased the surface area and electric current.

2. As the concentration and deposition time of gold nano-particles increased, the surface became rougher, and the electron transfer resistance was reduced.

3. When SAM was immobilized on the gold nano-particle-deposited electrode, the electron transfer rate from the redox reaction improved compared to the SAM-immobilized bare surface. Both cyclic voltammetry and electrochemical impedance spectroscopy verified it.

4. The density of the immobilized SAM was controlled to optimize the number of immobilized enzymes and electron transfer rate using reductive desorption method before binding the enzymes to the SAMs. Reductive desorption effectively eliminated MPA leaving TDT intact.

5. The ratio of two components, MPA and TDT, in the mixed SAMs affected the electron resistance and redox pattern in CV. The ratio of 80 : 20 showed less resistance and more distinct redox peaks than 50 : 50.

6. The HRP enzymes immobilized on the DTSP SAM showed clear redox behavior with 0.5 mM of H_2O_2 in a cyclic voltammogram.

7. HRP on the CV electrode followed the Michaelis-Menten equation, and the maximum rate and Michaelis-Menten constant were estimated I_{max}=833.33 nAmp, K_m=16.7 μM.

In summary, enzyme biosensors based on gold nano-particles and SAMs present several advantages with respect to stability, sim-

plicity, response time, and enzyme amount that could allow the rapid detection of enzyme substrates and inhibitors.

ACKNOWLEDGEMENTS

REFERENCES

1. P. W. Carr and L. D. Bowers, *Immobilized enzymes, in analytical chemistry: Fundamentals and applications*, Wiley, New York (1980).
2. A. E. G. Cass, G. Davis, G. D. Francis, H. A. O. Hill, W. J. Aston, I. J. Higgins, E. V. Plotkm, L. D. L. Scott and A. P. F. Turner, *Anal. Chem.*, **56**, 667 (1984).
3. X.-H. Wang and S. Wang, *Sensors*, **8**, 6045 (2008).
4. X. Lu, Z. Wen and J. Li, *Biomaterials*, **275**, 740 (2006).
5. D. Y. Yoon and D. S. Kim, *Korean J. Chem. Eng.*, **26**, 433 (2009).
6. H. Chen and Y. Zhang, *Proc. of the 10th Int. Conf. on Environ. Sci. & Technol.*, Kos island, Greece, 5-7 September (2007).
7. B. Serra, A. J. Reviejo and J. M. Pingarrón, *Electroanalysis*, **15**, 1737 (2003).
8. T. D. Dolidze, S. Rondinini, A. Vertova, D. H. Waldeck and D. E. Khoshtariya, *Biopolymers*, **87**, 68 (2007).
9. A. El Kasmi, J. M. Wallace, E. F. Bowden, S. M. Binet and R. J. Linderman, *JACS*, **120**, 225 (1998).
10. D. Hobara, S. Imabayashi and T. Kahiuchi, *Nano Lett.*, **2**, 1021 (2002).
11. M. C. Leopold and E. F. Bowden, *Langmuir*, **18**, 2239 (2002).
12. D. Hobara, Y. Uno and T. Kakiuchi, *Phys. Chem. Chem. Phys.*, **3**, 3437 (2001).
13. F. R. Shu and G. S. Wilson, *Anal. Chem.*, **48**, 1679 (1976).
14. R. A. Kamin and G. S. Wilson, *Anal. Chem.*, **52**, 1198, (1980).